Spatial behavior of squeezed states of light and quantum noise in optical images

M. I. Kolobov and I. V. Sokolov

Leningrad State University

It is shown that optical homodyne detection of monomode squeezed light can generate photon counting statistics that is regular not only in time but also in the plane of observation in which the counting process takes place. The characteristic spatial and spectral scales (in the language of spatial frequencies) of quantum-noise suppression are found. Methods of spatial modulation of a beam of light in a multimode squeezed state, i.e., methods of producing images with suppressed quantum noise are discussed. The transformation of the quantum statistics of multimode squeezed light propagating in empty space (i.e., during diffraction), and in optical systems (lenses) is examined. This may be of interest in connection with the transmission and processing of images containing noise below the shot level. Quantum-mechanical and energy estimates are given for low-noise observations, and the connection with holographic measurements is examined.

1. INTRODUCTION

The properties of squeezed states of light have attracted considerable attention in recent years not only because they have led to a re-examination of the fundamentals of quantum electrodynamics, but also because of the real possibility of low-noise optical measurement and communication. Squeezing in three-wave and four-wave parametric processes has frequently been observed in the optical range,[1-8] and there have been successful demonstrations of the quantum states of radiation in other physical phenomena.

Practically all the potential applications of squeezed states of radiation that have been examined so far rely on the possibility of producing (by optical homodyning) a beam of photons that is uniform in time when it is incident on an effective counter. The photoelectron emission times follow one another more regularly than independent photodetection events, and Poisson (shot) detection noise is suppressed. It may be considered that "one-dimensional" applications of squeezed states of light have now been fully investigated, including studies of physical processes and active methods of modulation in time.

Our aim here is to show that, under certain physical conditions that will be discussed below, squeezed light can give rise to photon-counting statistics that is regular not only in time, but also in space. The point is that we can identify the points in space at which photodetection events take place, i.e., observations are performed using a dense array of effective counters. This means that the homodyne reception of multimode squeezed beams of light can be used as a basis, at least in principle, for recording dynamic optical images and three-dimensional data sets with quantum noise suppressed below the Poisson level. This also applies to studies of physical processes distributed in both time and space.

In Secs. 4 and 6, we establish the spectral and space–time scales for the phenomenon of quantum noise suppression, i.e., we determine the resolving power of the measurements. We identify the main types of low-noise measurement that are possible for different types of phase matching (in the sense of frequency and angular degeneracy) of squeezed light.

In Sec. 5, we consider the wave propagation of squeezed light in empty space (diffraction) and in lens systems. We show that a thin lens can, in a certain specific sense, remove the spatial and frequency dispersion of multimode squeezed states and thus assure the best experimental spatial resolution.

In the concluding Sec. 6, we examine the limiting possibilities of multimode squeezed states from the standpoint of low-noise measurement, and provide quantum and power estimates. Existing methods of temporal control of a beam of squeezed light are extended to multimode squeezed states in space. The promising connection with holographic measurements is noted.

We have already mentioned that the literature devoted to squeezed states of light has been mostly concerned with the temporal behavior of these states (see the reviews in Refs. 9–11 and the special issue cited in Ref. 12). We note particularly Refs. 13–18 which discuss the spectral aspects (but only in relation to temporal behavior) of broad-band squeezing in degenerate three-wave interactions[17] in the case of parallel propagation (which is particularly close to our theme here) and in four-wave interactions in the case of anti-parallel propagation[15] and parallel propagation.[16] These and certain other publications have shown how the spectrum of intensity fluctuations in homodyne reception of a broad-band squeezed state is influenced by dispersion (i.e., frequency-dependent phase shifts of combining waves and the homodyne wave) in a parametric medium[17] or in an active resonator,[15] and on reflection by an external resonator.[16]

Biphoton emission[19-21] in spontaneous parametric scattering is intimately related to multimode states squeezed in space. Antibunching photocorrelations over the cross section of a light beam are important for noise suppression and have been noted in connection with resonant nonlinear diffraction.[22]

The behavior of the squeezed states of light in space is examined explicitly in Refs. 23–25. Free diffraction of light in a squeezed state produced in a monomode source of limited aperture is discussed in Ref. 23. Squeezed states of radiation can be produced in a medium whose electric and magnetic susceptibilities are arbitrary functions of position and

time. The space–time aspect of the resulting squeezing is discussed in a general form in Ref. 24, but without considering the question of observation.

The effect of diffraction on the properties of squeezed states of light during parametric generation is investigated in Ref. 25, and the connection between phase matching of conjugate waves and the squeezing efficiency is elucidated. In the present paper, we investigate, as in Ref. 25, the parametric mechanism of generation of squeezed states. Our conclusions on the angular dependence of the degree of squeezing are in agreement with the data reported in Ref. 25 in the limit of degenerate interactive parallel propagation.

Essentially new results such as the suppression of quantum noise during the writing and transmission of optical images, etc., are deduced below on the basis of a formulation of the problem of observation, which differs from the formulation adopted in the publications cited above. In our treatment, spatial fluctuations during homodyne detection are described by introducing the spectrum of intensity fluctuations that depends on both temporal and spatial frequencies.

2. DESCRIPTION OF SPACE AND TIME FLUCTUATIONS IN PHOTODETECTION

An optical image is the record of the number of photon counts (in a short interval of time in the case of a dynamic image or during the entire time of observation) as a function of the two-dimensional position vector $\rho = (y,z)$ on the plane of observation. In the continuous limit, one observes the surface current density $i(\rho,t)$, i.e., the specific count rate (per unit area per second) without multiplication by the charge of the electron.

The frequency and spatial-frequency spectrum $(i^2)_{q,\Omega}$ of the current density is a measure of the photodetection quantum noise:

$$(i^2)_{q,\Omega} = \int d\rho\, dt \exp[i(\Omega t - q\rho)]\left\langle \frac{1}{2}\{i(0,0), i(\rho,t)\}_+\right\rangle,$$

(1)

where $\{...,...\}_+$ represents the anticommutator. For a random process $i(\rho,t)$ that is stationary in both space and time, so that $\langle i(\rho,t)\rangle = \langle i\rangle$, the spectrum (1) determines the density of noise Fourier harmonics of the current density that are generated by given light.

For a classical light wave whose intensity is constant in both time and space, the expression given by (1) assumes the classical form, i.e., it is determined by the Poisson photon-counting statistics for which

$$(i^2)_{q,\Omega} \to \langle i\rangle.$$

(2)

We now extract from the positive-frequency part of the field $E(\mathbf{r},t)$ the fast component representing rays of frequency ω_h that propagate in the x direction (where $\mathbf{r} = (x,\rho)$):

$$E(x,\rho,t) = -i\xi\,(2\pi\hbar\omega_h)^{1/2}\exp[i(k_h x - \omega_h t)]e(x,\rho,t).$$

(3)

In a parametric crystal, the factor ξ depends on the type of polarization and the branch of lattice oscillations in the crystal[19] (in vacuum, $\xi = 1$). The wave number k and frequency ω are connected by the dispersion relation of the crystal[1)]

$(k \to k^{(0)} = \omega/c$ in empty space). The expectation value $\langle e^+(x,\rho,t)e(x,\rho,t)\rangle$ is the energy density per unit volume, scaled by $\hbar\omega_h$.

Let us suppose that the plane of photodetection intersects the longitudinal axis of coordinates at a point x outside the crystal. For near-normal illumination, the theory of photodetection (see Ref. 11) shows that the dependence of the current density and its correlation function on the field strength is

$$\langle i(\rho, t)\rangle = \eta c\langle e^+(x, \rho, t)e(x, \rho, t)\rangle,$$

$$\langle \tfrac{1}{2}\{i(\rho_1, t_1), i(\rho_2, t_2)\}_+\rangle = \langle i(\rho_1, t_1)\rangle\delta(\rho_{21})\delta(t_{21})$$

$$+\eta^2 c^2\{\langle e^+(x, \rho_1, t_1)e^+(x, \rho_2, t_2)$$

$$\times e(x, \rho_2, t_2)e(x, \rho_1, t_1)\rangle\theta(t_{21})+(1\leftrightarrow 2)\},$$

(4)

where η is the detection quantum yield, $\eta \lesssim 1$, $\theta(t)$ is the step function, $t_{21} = t_2 - t_1$, and $\rho_{21} = \rho_2 - \rho_1$. The Poisson limit (2) is produced by the first (shot) contribution to the current autocorrelator (4).

3. FREQUENCY AND SPATIAL-FREQUENCY SPECTRUM OF FLUCTUATIONS IN THE INTENSITY OF SQUEEZED LIGHT

Consider the three-wave parametric interaction in a crystal of thickness l (a plane slab perpendicular to the x axis; see Fig. 1). A plane monochromatic pump wave of frequency $\omega_p = 2\omega_h$ is incident on this slab at right angles to its surface. As a result of scattering, a pump photon ω_p splits into two PS photons with frequencies $\omega_h + \Omega$ and $\omega_h - \Omega$ and wave vectors $\mathbf{k}(\mathbf{q},\Omega)$ and $\mathbf{k}(-\mathbf{q}, -\Omega)$. Let $\mathbf{k}(\mathbf{q},\Omega)$ represent the wave vector of the PS photon of frequency $\omega_h + \Omega$ in the crystal, with transverse component $\mathbf{q}$. The frequency Ω and the spatial frequency $\mathbf{q}$ are conserved in the scattering process because it is stationary and transversely homogeneous. The parametric interaction occurs effectively at the frequencies $\mathbf{q}, \Omega$ for which the phase-matching condition is satisfied, i.e., the wave mismatch $\Delta(\mathbf{q},\Omega)$ is small:

$$\Delta(\mathbf{q}, \Omega)l \lesssim 1, \quad \Delta(\mathbf{q}, \Omega) = k_x(\mathbf{q}, \Omega) + k_x(-\mathbf{q}, -\Omega) - k_p,$$

(5)

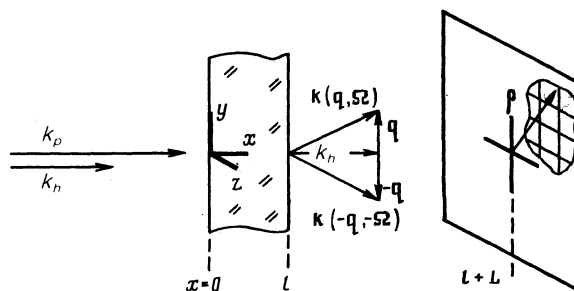where k_p is the pump wave number in the crystal.

FIG. 1. Generation and homodyne photodetection of multimode squeezed states of light. Part of the dense array of photodetectors with independent outputs is indicated in the plane of observation $x = l + L$ ($L \to 0$ in Secs. 3 and 4).

A plane wave of frequency ω_h (the homodyne wave) is also incident normally on the slab (on the same side) and produces beats with the PS waves in the plane of detection. The development of the PS waves and the homodyne in the crystal is described by[19-26]

$$\partial \varepsilon (x, \mathbf{q}, \Omega)/\partial x = \sigma \varepsilon^+ (x, -\mathbf{q}, -\Omega)\exp\{-i\Delta(\mathbf{q}, \Omega)x\}, \qquad (6)$$

where

$$\varepsilon (x, \mathbf{q}, \Omega) = e(x, \mathbf{q}, \Omega)\exp\{-i[k_x(\mathbf{q}, \Omega)-k_h]x\}. \qquad (7)$$

The constant σ is proportional to the amplitude of the classical pump wave (pump depletion is ignored). From (6) and (7) we have the transformation of the slow Fourier component $e(x,\mathbf{q},\Omega)$ between entry $(x = 0)$ and exit $(x = l)$:

$$e(l, \mathbf{q}, \Omega) = U(\mathbf{q}, \Omega)e(0, \mathbf{q}, \Omega) + V(\mathbf{q}, \Omega)e^+(0, -\mathbf{q}, -\Omega), \qquad (8)$$

where

$$U(\mathbf{q}, \Omega) = \exp\{i[k_x(\mathbf{q}, \Omega)-k_\Gamma-\Delta/2] l\} [\text{ch}(\gamma l)$$
$$+ (i\Delta/2\gamma)\text{sh}(\gamma l)],$$

$$V(\mathbf{q}, \Omega) = \exp\{i[k_x(\mathbf{q}, \Omega)-k_h-\Delta/2]l\}(\sigma/\gamma)\text{sh}(\gamma l) \qquad (9)$$

in which $\Delta = \Delta(\mathbf{q},\Omega)$, $\gamma = (|\sigma|^2 - \Delta^2/4)^{1/2}$ because of the unitarity condition $|U|^2 - |V|^2 = 1$. On entry to the crystal in vacuum, the operators $e(0,\mathbf{q},\Omega)$ satisfy the free-field commutation relations

$$[e(0, \mathbf{q}_1, \Omega_1), e^+(0, \mathbf{q}_2, \Omega_2)] = (2\pi)^3 c^{-1}\delta(\mathbf{q}_2-\mathbf{q}_1)\cdot\delta(\Omega_2-\Omega_1). \qquad (10)$$

The initial quantum state of the field $|in\rangle$ is the vacuum state, except for the homodyne wave whose state on entry into the slab is coherent and has the complex amplitude α

$$e(0, \boldsymbol{\rho}, t)|in\rangle = \alpha|in\rangle. \qquad (11)$$

The amplitude of the homodyne wave at entry to the crystal is[2]

$$\beta = |\beta|\exp(i\varphi_\beta) = \alpha U(0, 0) + \alpha^* V(0, 0). \qquad (12)$$

The mean current density $\langle i\rangle$ is determined by the intensities of the homodyne and PS waves. From (4) and (8)-(12), we have

$$\langle i\rangle = c\eta|\beta^2| + \eta(2\pi)^{-3}\int dq\, d\Omega\,|V(\mathbf{q}, \Omega)|^2 = \langle i\rangle_h + \langle i\rangle_{\text{PS}}. \qquad (13)$$

Let us now introduce the degeneracy parameter $\delta_{q,\Omega}$ for the PS waves, where $\delta_{q,\Omega} \equiv |V(\mathbf{q},\Omega)|^2$. This parameter is equal to the mean number of photons within the coherence volume. The mean current density due to parametric scattering can be written in the form

$$\langle i\rangle_{\text{PS}} \sim (2\pi)^{-3}q_c^2\Omega_c\bar{\delta}_{q,\Omega} \sim \bar{\delta}_{q,\Omega}/S_c T_c, \qquad (14)$$

where $T_c \sim 2\pi/\Omega_c, S_c \sim (2\pi/q_c)^2$ are, respectively, the PS coherence time and area, determined in terms of the widths Ω_c and q_c of the frequency and spatial-frequency spectrum of the field. The bar over δ denotes an average over the frequencies of $\mathbf{q},\Omega$, as defined by (13), within the PS spectrum.

To find the noise spectrum of the photocurrent density (1), we must evaluate the current autocorrelator (4) with the field solutions (8) and (9). The quantum-mechanical averaging is performed over the initial state of the field $|in\rangle$, using (10)-(12). The final result is

$$(i^2)_{\mathbf{q},\Omega} = \langle i\rangle + \eta^2\Big\{ 2|\beta|^2 c[\delta_{\mathbf{q},\Omega} + \text{Re}(\exp(-2i\varphi_\beta)g(\mathbf{q},\Omega))]$$

$$+ (2\pi)^{-3}\int dq'\, d\Omega'[\delta_{q',\Omega'}\delta_{q-q',\Omega-\Omega'}$$

$$+ g^*(q',\Omega')g(q-q',\Omega-\Omega')]\Big\}, \qquad (15)$$

where $g(\mathbf{q},\Omega) = U(\mathbf{q},\Omega)V(-\mathbf{q},-\Omega)$. The spectrum is given for $\mathbf{q},\Omega \neq 0$, i.e., it describes noise. The first term in (15) corresponds to the shot noise. The contribution of beats between the homodyne and the PS waves is proportional to the homodyne intensity $|\beta|^2$ and depends on the choice of its phase φ_β (relative to the pump wave). There is also a contribution due to the self-beats of the PS waves which, in spectral language, describes the bunching of photons in PS.

4. SUPPRESSION OF INTRINSIC FLUCTUATIONS IN HOMODYNE DETECTION OF SQUEEZED LIGHT AS A FUNCTION OF THE TYPE OF PHASE MATCHING

The question of phase matching in parametric interactions has now been investigated from various points of view. The spectral, angular, and power characteristics of radiation,[19,26] photon correlations in the absence of the homodyne wave,[19-21] and squeezing efficiency[25] have all been examined.

In this section, we investigate in detail the intensity fluctuation spectrum (15) and show that different types of phase matching during the generation of squeezed light select particular types of low-noise observation. We give criteria for choosing the phase matching for a particular measurement, and determine the spectral and spatial-temporal scales governing the resolving power in such measurements.

We begin by introducing the phase and amplitude squeezing parameters for observations directly on the exit face:

$$\psi(l, \mathbf{q}, \Omega) = \tfrac{1}{2}\arg\{U(\mathbf{q}, \Omega)V(-\mathbf{q}, -\Omega)\}, \quad \exp[\pm r(\mathbf{q}, \Omega)]$$
$$= |U(\mathbf{q}, \Omega)| \pm |V(\mathbf{q}, \Omega)|. \qquad (16)$$

Their physical significance for multimode squeezing becomes apparent when we consider noise modulation of the strong homodyne wave by the squeezed phase-conjugate waves $(\mathbf{q},\Omega)$ and $(-\mathbf{q}, -\Omega)$ from the continuous PS spectrum. Generalizing the conclusions of Ref. 14 (where the analysis was confined to temporal modulation) to noise modulation in both space and time, we may conclude as follows.

(1) In the complex plane of the amplitude $e(l,\boldsymbol{\rho},t)$, i.e., in the plane of the quadrature components, the fixed homodyne mean-field vector β adds to the resultant vector $\delta e(l,\boldsymbol{\rho},t)$ of the two phase-conjugate waves which oscillate in time with frequency Ω and in space with frequency $\mathbf{q}$ (as a function of displacement in the plane of observation).

(2) The uncertainty relation shows that the noise motion at frequencies $\mathbf{q}$, Ω occurs on average inside the uncer-

M. I. Kolobov and I. V. Sokolov   1099

tainty ellipse whose semimajor axis is at the angle $\psi(l,\mathbf{q},\Omega)$. The semimajor axis of the ellipse increases when the squeezed state appears, whereas the semiminor axis decreases as $\exp[\pm r(\mathbf{q},\Omega)]$.

(3) The form of the noise modulation of the resultant field in space and in time with frequencies $\mathbf{q}$, Ω is determined by the angle $\theta(\mathbf{q},\Omega) = \psi(l,\mathbf{q},\Omega)$ by which the squeezed light ellipse is rotated relative to the homodyne. Phase modulation predominates for $\theta(\mathbf{q},\Omega) \sim \pm \pi/2$ and amplitude modulation for $\theta(\mathbf{q},\Omega) \sim 0,\pi$.

Assuming a high-intensity homodyne, and discarding temporarily the contribution of the PS waves to shot noise and to the self-beats, we can reduce the spectrum (15) to the form

$$(i^2)_{\mathbf{q},\,\mathrm{\Omega}} = \langle i \rangle_h \{1 - \eta + \eta [\cos^2(\theta(\mathbf{q},\ \Omega))\exp(2r(\mathbf{q},\ \Omega))$$
$$+ \sin^2(\theta(\mathbf{q},\ \Omega))\exp(-2r(q,\ \Omega))]\}, \qquad (17)$$

where the degree of squeezing is related to the degeneracy parameter $\delta_{\mathbf{q},\Omega}$, i.e., the intensity, of the PS waves. By virtue of (9) and (16), and the definition of $\delta_{\mathbf{q},\Omega}$ this is described by

$$\exp r(\mathbf{q},\Omega) = (1 + \delta_{\mathbf{q},\mathrm{\Omega}})^{1/2} + \delta_{\mathbf{q},\mathrm{\Omega}}^{1/2}. \qquad (18)$$

The spectral power density of fluctuations at frequencies $\mathbf{q},\Omega$ is determined by the projections of the noise motions of the field along the axes of the squeezing ellipse onto the amplitude of the homodyne. The dispersion of the uncertainty ellipse, i.e., the frequency dependence of the noise modulation as specified by (9) and (16), is shown in Fig. 2. The contribution $\langle i \rangle_h (1 - \eta)$ describes the partial restitution of Poisson noise in nonideal photon counting.

Maximum squeezing occurs at frequencies $\mathbf{q}_s,\Omega_s$ that belong to the phase matching surface in $\{\mathbf{q},\Omega\}$ space, which is defined by the condition $\Delta(\mathbf{q}_s,\Omega_s) = 0$. We then have $r(\mathbf{q}_s,\Omega_s) \equiv r_s = |\sigma|/l$. The phase of the homodyne is chosen in accordance with the condition $\theta(\mathbf{q}_s,\Omega_s) = \pm \pi/2$ that ensures the predominance of phase noise modulation near the phase matching surface. The intensity fluctuations near this surface are found to be suppressed to the highest extent:

$$(i^2)_{\mathbf{q}_s,\mathrm{\Omega}_s} = \langle i \rangle_h \{1 - \eta + \eta \exp(-2r_s)\} \xrightarrow[\eta \to 1]{} \langle i \rangle_h \exp(-2r_s).$$

$$(19)$$

The spectral range of noise suppression is determined by the frequency and space–time suppression of squeezing. For small scattering angles, i.e., for $q/k_h \ll 1$, the projection of the wave vector $\mathbf{k}(\mathbf{q},\Omega)$ onto the x axis is

$$k_x(\mathbf{q},\ \Omega) \approx k(\Omega) [1 - q^2/2k^2(\Omega)].$$

In the quadratic approximation in frequency ($\Omega/\omega_h \ll 1$) the wave detuning is given by

$$\Delta(\mathbf{q},\ \Omega) \approx \Delta(0,\ 0) + k_\mathrm{\Omega}''(0)\Omega^2 - q^2/k_h, \quad \Delta(0,\ 0) = 2k_h - k_p.$$

$$(20)$$

We can now use (9) to verify that, for large squeezing, i.e., for $r_s \gg 1$, the quantities $r(\mathbf{q},\Omega)$ and $\theta(\mathbf{q},\Omega)$ near the phase-matched state have the form

$$r(\mathbf{q},\ \Omega) \approx r_s, \quad \theta(\mathbf{q},\ \Omega) \approx \theta(\mathbf{q}_s,\ \Omega_s) + \Delta(\mathbf{q},\ \Omega)l_{\mathrm{amp}}/4, \qquad (21)$$

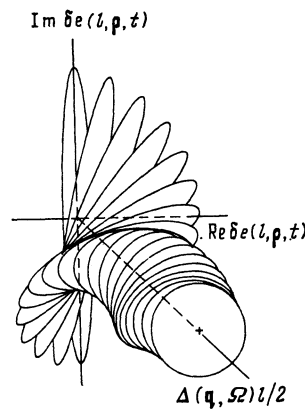FIG. 2. Dispersion (dependence on frequencies $\mathbf{q},\Omega$) of the squeezing ellipse at exit from the parametric crystal for $\exp(2r_s) = 10$. The dimensionless wave detuning $\Delta(\mathbf{q},\Omega)l/2$ is shown in steps of 0.32 and is compared with the complex planes on which the squeezing ellipse is shown for the conjugate waves $(\mathbf{q},\Omega)$ and $(-\mathbf{q},-\Omega)$.

where $l_{\mathrm{amp}} = |\sigma|^{-1}$ is the characteristic parametric amplification length. The approximation defined by (21) is valid for frequencies for which $|\Delta(\mathbf{q},\Omega)l_{\mathrm{amp}}| \ll 1$. As we depart from the phase-matching surface $(\mathbf{q} \neq \mathbf{q}_s, \Omega \neq \Omega_s)$, the squeezing ellipse rotates, initially retaining its dimensions. In the case $\theta(\mathbf{q}_s,\Omega_s) \neq \pm \pi/2$, the homodyne begins to beat with the "noisy" quadrature component of the PS field.

Let us now consider frequency and angle degenerate matching ($\Delta(0,0) = 0$), for which PS photons have close frequencies and are mostly emitted in forward directions $\Omega \sim 0, q \sim 0$. In view of (20) and (21), the noise spectrum of the photocurrent density near the matching surface assumes the following form for optimum tuning $\theta(\mathbf{q}_s,\Omega_s) = \pm \pi/2$:

$$(i^2)_{\mathbf{q},\,\mathrm{\Omega}} \approx \langle i \rangle_h \{1 - \eta + \eta [(\mathrm{sign}\ k_\mathrm{\Omega}''(0))\Omega^2/\Omega_p{}^2 - q^2/q_p{}^2)^2$$

$$+ \exp(-2r_s)]\}, \qquad (22)$$

where

$$\Omega_p = 2(|k_\mathrm{\Omega}''(0)|l_{\mathrm{amp}}\exp r_s)^{-1/2},$$
$$q_p = 2(k_h^{-1}l_{\mathrm{amp}}\exp r_s)^{-1/2}$$

Figure 3a shows the typical noise spectrum (17) for these conditions (it is assumed that $k_\mathrm{\Omega}''(0) < 0$.[3] It is clear from (22) and from this figure that the photocurrent density fluctuations in the region $q < q_p, \Omega < \Omega_p$ are smaller than the shot fluctuations. In space–time language, this can be interpreted as follows (cf. Sec. 6 which gives a quantitative analysis for the optimum lens experiment). Suppose that the photoelectrons are collected from a portion of the surface $\Delta S \gtrsim S_p = (\pi/q_p)^2$ for a time $\Delta T \gtrsim T_p = \pi/\Omega_p$. Fluctuations in the number of photoelectrons are determined by the low-frequency harmonics of the current density noise, such that $q \lesssim q_p, \Omega \lesssim \Omega_p$, and the high frequencies do not contribute because of averaging over the collection surface during the acquisition time. However, since noise is suppressed at low frequencies, the mean square fluctuations in the number of collected photoelectrons is less than the Poisson value. Thus, the frequencies Ω_p, q_p found above deter-
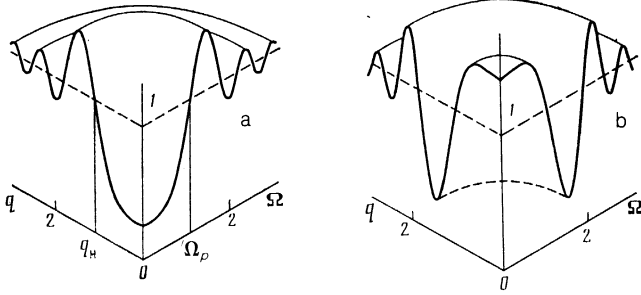
M. I. Kolobov and I. V. Sokolov   1100

FIG. 3. Spectrum of current density fluctuations $(i^2)_{q,\Omega}$: a—phase matching degenerate in angle and frequency $\Delta(0,0) = 0, k''_\Omega(0) < 0$, b—$\Delta(0,0) > 0$, c—$k''_\Omega(0) < 0$. The spectrum plotted along the vertical axis is shown relative to the shot level $\langle i \rangle$; the frequency Ω and the spatial frequency q are given in units of $(|k''_\Omega(0)|l/2)^{-1/2}$ and $(2k_h/l)^{1/2}$, respectively. The degree of squeezing corresponds to $\exp r_s = 2, \eta = 1$.

mine the minimum time T and the area S_p over which photons are collected with reduced level of noise at exit from the nonlinear crystal. Note that the factor $(l_{amp}/k_h)^{1/2}$ in the linear size of the low-noise detection area is due to wave propagation in the crystal: diffraction spreading of this size over the length l_{amp} is of the order of the size itself.

There is both physical and practical interest in low-noise measurements when (a) the useful information in the dynamic image is "concentrated" near nonzero carrier frequencies q and Ω, i.e., a space–time spectral analysis must be carried out near these frequencies, (b) a spectral analysis of the image is required only for the spatial variable near the carrier frequency q, and there is no need for a spectral analysis with respect to time, and (c) a spectral analysis with respect to time is required, but the spatial analysis is not.

These measurements can be made for phase-matched waves that are nondegenerate in frequency and angle during the generation of squeezed light, for example, for $\Delta(0,0) > 0, k''_\Omega(0) < 0$. The characteristic noise spectrum (17) for this case is shown in Fig. 3b (optimal tuning of the homodyne phase). The matched region is shown by the dashed line. For the measurements that we have just enumerated, we have to take a nonlinear medium and an experimental geometry that will ensure that the phase-matching surface, i.e., noise suppression region, will cross the carrier frequencies: (a) $q \neq 0$, $\Omega \neq 0$, (b) $q \neq 0$, $\Omega = 0$, (c) $q = 0$, $\Omega \neq 0$. Other varieties of wave matching can be described in a similar way (for example, $k''_\Omega(0) > 0$).

To conclude this section, let us estimate the homodyne intensity necessary to ensure that the contribution of self-beating and of the shot component associated with parametric scattering are not significant for the problem of homodyne detection noise. Suppose that the homodyne is turned off, $\beta \to 0$. The spectrum (15) then consists of self-beats and the PS shot noise. We confine our attention to the angle and frequency degenerate case $\Delta(0,0) = 0$. At low frequencies,

$$(i^2)_{0,0} = \langle i \rangle_{PS} (1+\eta) + 2\eta^2 (2\pi)^{-3} \int d\mathbf{q} \, d\Omega \, \delta_{q,\Omega}, \quad (23)$$

where we have used the fact that $|U|^2 - |V|^2 = 1$ and that $g(\mathbf{q},\Omega), \delta_{q,\Omega}$ are even quantities. In the first approximation, we replace one factor in (23) with $\delta_{0,0}$ and use the definition of $\langle i \rangle_{PS}$ given by (13). This gives

$$(i^2)_{0,0} \sim \langle i \rangle_{PS} \{1+\eta+2\eta\delta_{0,0}\}. \quad (24)$$

The contribution of the term $\langle i \rangle_{PS} (1 + \eta)$ is corpuscular in character and is due to noise in the detection of pairs of simultaneously emitted PS photons (biphotons).[19] If squeezing is effective, i.e., PS is degenerate, (24) is dominated by wave noise ($\sim \delta_{0,0}$). The spectral power of self-beats and of the shot component of parametric scattering is not significant even at the noise minimum during effective squeezing and homodyning, provided the homodyne intensity is high enough:

$$\langle i \rangle_h \{1 - \eta + \eta \exp(-2r_s)\} \gg \langle i \rangle_{PS} (1+\eta+2\eta\delta_{0,0}). \quad (25)$$

5. EFFECT OF FREE PROPAGATION AND FOCUSING IN A SQUEEZED STATE ON PHOTODETECTION FLUCTUATIONS

The aim of this section is to extend the above conclusions about low-noise measurement in spatially multimode squeezed light by taking into account free transfer and wavefront control by a thin lens. We show that the resolving power is reduced by diffraction in the case of free wave propagation. We establish the following important property of lens systems and systems similar to them: it is possible to compensate the spatial and frequency dispersion of the phase of a multimode squeezed state, which is produced during the propagation of light in the crystal (during generation) and in the vacuum on the way to the detector. This means that a thin lens can be used to restore the resolving power of low-noise measurement to its limiting value.

In contrast to the preceding sections, we shall now assume that the plane of detection lies at a distance L from the exit face of the nonlinear crystal and is parallel to it. In the case of free radiation transfer from a plane l to the plane $l + L$ we have

$$e(l+L, \mathbf{q}, \Omega) = \exp\{i(k_x^{(0)}(\mathbf{q}, \Omega) - k_h^{(0)})L\}e(l, \mathbf{q}, \Omega). \quad (26)$$

The observed field is related to the wave incident on the crystal by the squeezing transformation [see (8) and (26)]:

$$e(l+L, \mathbf{q}, \Omega) = \bar{U}(\mathbf{q}, \Omega)e(0, \mathbf{q}, \Omega) + \bar{V}(\mathbf{q}, \Omega)e^+(0, -\mathbf{q}, -\Omega), \quad (27)$$

where

$$\bar{U}(\mathbf{q}, \Omega) = \exp\{i(k_x^{(0)}(\mathbf{q}, \Omega) - k_h^{(0)})L\} U(\mathbf{q}, \Omega), \quad (28)$$

and the quantities $\bar{V}$ and V are similarly related. As in Sec. 4, we consider the squeezing parameters $\bar{r}(\mathbf{q},\Omega)$ and $\bar{\theta}(\mathbf{q},\Omega)$. It is readily seen that, in the case of free propagation from $x = l$ to $x = l + L$, the degree of squeezing remains unaltered, $\bar{r}(\mathbf{q},\Omega) = r(\mathbf{q},\Omega)$, and the squeezing ellipse rotates relative to the complex amplitude of the homodyne by the angle

$$\bar{\theta}(\mathbf{q}, \Omega) = \theta(\mathbf{q}, \Omega) + [k_x^{(0)}(\mathbf{q}, \Omega) + k_x^{(0)}(-\mathbf{q}, -\Omega)$$
$$- 2k_h^{(0)}]L/2 \approx \theta(\mathbf{q}, \Omega) - q^2 L/2k_h^{(0)}, \quad (29)$$

where it is assumed that $q/k_h^{(0)} \ll 1$ (paraxial approximation) and $\Omega/\omega_h \ll 1$. It is clear that free transfer enhances the dependence of the angle $\bar{\theta}(\mathbf{q},\Omega)$ on the spatial frequency. In a figure analogous to Fig. 2, this would appear as a fast turning over and a rotation of the squeezing ellipse with increasing q. From the standpoint of modulation, conjugate PS

waves traveling at an angle $\sim q/k_h^{(0)}$ and the homodyne wave that they modulate have different phase shifts, so that the phase and amplitude modulation of the resultant field are found to replace one another periodically in space. The oscillations shown in Fig. 4 are also found to appear in the spectrum of $(i^2)_{q,\Omega}$.

Let us now estimate the area of low-noise detection, taking diffraction over the length L into account. So long as the rotation of the squeezing ellipse is small, $|\theta(\mathbf{q},\Omega) - \theta(\mathbf{q}_s,\Omega_s)| \ll 1$, the expansion given by (21) is valid and, using (29), we find that

$$\bar{\theta}(\mathbf{q},\ \Omega) \approx \theta(\mathbf{q}_s,\Omega_s)$$
$$+ [\Delta(0,0) + k\Omega''(0)\Omega^2]l_{yc}/4 - q^2\,(l_{amp}/4k_h + L/2k_h^{(0)}),$$

(30)

where the amplification length has been combined with the mean free path. For angle and frequency degenerate matching, we can use the low-noise detection area estimated in Sec. 4 with $l_{amp}/k_h \rightarrow l_{amp}/k_h + 2L/k_h^{(0)}$. For $L \gg l_{amp}$, this area is determined by diffraction phenomena over the length L, and increases with increasing distance to the plane of detection.[4] However, this deterioration in resolving power is entirely due to the phase shift experienced by the light waves during propagation in vacuum, and is therefore reversible. More than that, and as we shall presently show, the phase shifts produced in the nonlinear crystal can also be compensated, and this can be used, at least in principle, to achieve the limiting spatial resolution.

Suppose that a lens of focal length f is inserted into the light beam so that its center lies along the longitudinal axis ($\rho = 0$). The thin lens "multiplies" the complex amplitude of the monochromatic wave by the factor $\exp[-ik^{(0)}(\Omega)\rho^2/2f]$, i.e., it introduces a phase shift (the finite aperture of the lens is not taken into account). The field is transferred from the plane x to the plane $x + 4f$ (the lens lies in the plane $x + 2f$) in accordance with the expression

$$e(x+4f,\ \boldsymbol{\rho},\ t) = \exp(ik_h^{(0)}\rho^2/2f)\,e(x,\ -\boldsymbol{\rho},\ t-(4f+\rho^2/2f)/c).$$

(31)

Note that the spectrum of $(i^2)_{q,\Omega}^{(x+4f)}$, which corresponds to observation in the plane $x + 4f$ behind the lens, and the spectrum of $(i^2)_{q,\Omega}^{(x)}$, which describes observation in front of the lens in the plane x, are identical. Actually (31) leads to the following conclusions.

(1) The phase factor $\exp(ik_h^{(0)}\rho^2/2f)$ has no effect on the light intensity and cancels out in the photodetection relations given by (4).

(2) The time delay is constant for $f \gg \rho$ in the region of the observation, and has no effect on the spectrum of the stationary process $i(\boldsymbol{\rho},t)$.

(3) The imaging $\boldsymbol{\rho} \rightarrow -\boldsymbol{\rho}$ has no effect on the spectrum (1) if it is even in the spatial frequency $\mathbf{q}$, which is indeed the case (we recall that the anisotropy of the PS waves is not taken into account).

If the lens and the plane of observation are arranged as indicated above, and for $x = l$ (exit face), the noise spectrum observed in the plane $l + 4f$ is identical with the spectrum recorded at exit from the crystal (as described in the last few sections). This is not surprising: the low-noise detection area, which we can envision on the exit face, is imaged by the lens on the "conjugate" area on the detector.

Less obvious (though advantageous) is the possibility of taking $x = l + L$ where, so far, L is arbitrary. The transfer of the field from the exit plane l to the plane of observation, $l + L + 4f$, is now described as transfer in vacuum over a distance L, where the sign of L is unimportant because (26) is also valid for "backward transfer" ($L < 0$) and for the imaging (31) by the lens, which does not involve the spectrum of intensity fluctuations. The observed spectrum should be identical with the spectrum found with allowance for only the free transfer over the length L. All that remains is to arrange the observations so that the condition $l_{amp}/k_h + 2L/k_h^{(0)} = 0$ is satisfied, i.e., the lens images a plane in the interior of the crystal ($L < 0$) on the surface of the detector, and the observed spectrum is unaffected by spatial and frequency dispersion of the angle $\bar{\theta}(\mathbf{q},\Omega)$ (for small deviations, $|\theta(\mathbf{q},\Omega) - \theta(\mathbf{q}_s,\Omega_s)| \ll 1$).
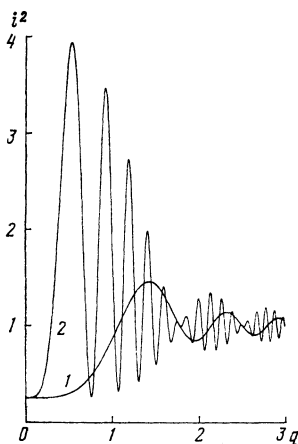

FIG. 4. Current density spectrum $(i^2)_{q,\Omega=0}$ observed at exit from the crystal (curve 1) and at a distance $L = 7l_{amp}k_h^{(0)}/2k_h$ from it (curve 2). Phase matching degenerate in frequency and angle, $(\bar{\theta}(0,0) = \pm\pi/2/\exp r_s = 2, \eta = 1$. The spectrum is shown relative to the shot noise $\langle i \rangle$ and q is in units of $(2/k_h/l)^{1/2}$.
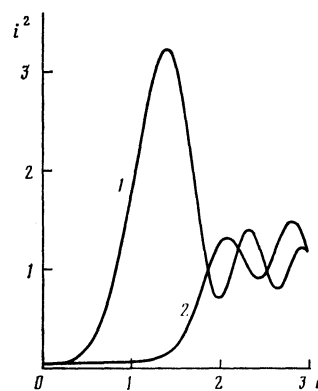

FIG. 5. The effect of a thin lens on the current density spectrum $(i^2)_{q,\Omega=0}$. Curve 1—observation at exit from the crystal, curve 2—observation with compensation of the dispersion of the squeezing angle by the lens; $\exp r_s = 5, \eta = 1$. The spectrum is shown relative to the shot noise $\langle i \rangle$, and q is in units of $(2k_h/l)^{1/2}$.

M. I. Kolobov and I. V. Sokolov   1102

Actually, this means that the expression given by (30) no longer depends on the spatial frequency. In the experiment with the lens, the squeezing ellipses can be identically oriented (cf. Fig. 2), at least near the phase-matching surface, where the degree of squeezing is at a maximum.

It is noted in Ref. 25 that the squeezing efficiency is greater when the light waves are focused on the nonlinear medium. The consequences of energy concentration,[27] and the separation of conjugate waves in space[28] during focusing, have been discussed in the literature. In our case, focusing means controlling noise modulation of the resultant field independently of the nonlinear medium (in contrast to Ref. 25) and is unrelated to energy concentration or the spatial separation of the biphotons (in contrast to Refs. 27 and 28).

Figure 5 shows the spatial-frequency spectrum of current density fluctuations for observations at exit from the crystal and in the optimum case of observation with the lens (angle and frequency degenerate matching; $\tilde{\theta}(0,0) = \pm \pi/2$). The photodetection quantum noise is suppressed practically throughout the spatial-frequency band of the degenerate PS, and this determines the resolving power, and the bottom of the valley in the noise spectrum tends to become flat.

To improve the frequency behavior of the noise spectrum as well, we must introduce additional frequency-dependent phase shifts for the PS and homodyne waves. It can be shown that, if we insert a layer of matter of length $l^{(1)}$, and the required sign of $k_\Omega^{(1)''}(0)$, into the light beam ($k^{(1)}$ is the wavenumber), and if

$$k_\Omega''(0)\, l_{\mathrm{amp}}/2 + k_\Omega^{(1)''}(0)\, l^{(1)} = 0 , \qquad (32)$$

the frequency dependence of the angle $\tilde{\theta}(q,\Omega)$ is also compensated.

Thus, multimode squeezed light retains (and sometimes improves) its ability to suppress quantum noise in measurements with optical devices such as lenses.

6. PHYSICAL POSSIBILITIES OF MEASUREMENT AND DATA TRANSMISSION WITH LOW QUANTUM NOISE IN SPACE AND IN TIME

Let us now summarize our discussion and give the final estimates for the spectral, space-time, and power characteristics of measurements in squeezed light.

When the dependence of the angular squeezing parameter on the frequencies q,Ω (see above) is compensated, the photodetection noise is suppressed virtually across the entire spectral region $q \langle q_c/2, \Omega \langle \Omega_c/2$ in which there is well-defined (degenerate) parametric scattering.[5] We must now determine the mean square fluctuation in the number $N_{\Delta S, \Delta T}$ of photoelectrons counted over an area $\Delta S = \Delta y \Delta z$ during the time ΔT. We do this by comparing the observed $N_{\Delta S, \Delta T}$ with the integral of the current density $i(\rho, t)$ with respect to area and time. When we evaluate the average $N^2_{\Delta S, \Delta T}$, we can express the current density autocorrelator in terms of the known spectrum (1) and (15) of the current density [cf. Ref. 11]. It is readily shown that

$$\langle \delta N^2_{\Delta S, \Delta T} \rangle = \langle N_{\Delta S, \Delta T} \rangle$$

$$\times \int dq\, d\Omega\, \tilde{\delta}_{1/\Delta T}(\Omega)\, \tilde{\delta}_{1/\Delta y}(q_y)\, \tilde{\delta}_{1/\Delta z}(q_z)\, (i^2)_{q,\Omega} \langle i \rangle^{-1},$$

$$(33)$$

where the step functions $\tilde{\delta}$ are defined by

$$\tilde{\delta}_{1/\Delta T}(\Omega) = 2 \sin^2(\Omega \Delta T/2)/\pi \Omega^2 \Delta T. \qquad (34)$$

According to (33) and (34), the mean square fluctuation in the photon counts is determined by the noise spectral density at low frequencies, $q \lesssim q_c/2, \Omega \lesssim \Omega_c/2$, where $(i^2)_{q,\Omega} \langle i \rangle^{-1} \to 1 - \eta + \eta \exp(-2r_s) < 1)$, provided $\min(\Delta y, \Delta z) \gtrsim 2\pi/q_c, \Delta T \gtrsim 2\pi/\Omega_c$ is then sub-Poissonian. The order of magnitude of the minimum area and of the minimum time of low-noise measurement are therefore determined by the PS coherence area S_c and coherence time T_c.

The average number of PS photons and homodyne photons necessary for a single low-noise measurement ($\Delta S = S_c, \Delta T = T_c$) is therefore $\langle i \rangle_{\mathrm{PS}} S_c T_c \sim \tilde{\delta}_{q,\Omega}$ and $\langle i \rangle_h S_c T_c$, respectively [cf. (14) and (15)].

If the pump and homodyne waves illuminate a spot of area $S \gg S_c$ on the nonlinear crystal, the number of low-noise measurements that can be made in the squeezed light in a time $T \gg T_c$ is $ST/S_c T_c \gg 1$, which is equivalent to transmitting $T/T_c \gg 1$ images consisting of $S/S_c \gg 1$ "elements" each. The source of squeezed states that we have investigated generates S/S_c spatial modes of radiation, which basically distinguishes it from the monomode source employing a resonator or waveguide (see Ref. 23 and numerous other papers).

We must now consider some possible physical methods of controlling multimode squeezed light, which do not introduce additional noise. A screen containing apertures can be used for binary modulation in space. As shown above, collection of photons on the apertures ($\Delta S \gtrsim S_c$) will be a low-noise process, and there will be no photon counts on the opaque areas, i.e., no noise. Another method of imaging involves weak nonuniform absorption. The noise introduced in this way can be estimated from (19) in which absorption can be simulated by a reduction in the quantum yield η.

The displacement of multimode squeezed light beams by interference is also of interest (and awaits investigation), since this method of modulation has already been evaluated[29,30] for "one-dimensional," spatially monomode, light fields with quantum statistics.

Both methods are promising in connection with studies of the spatial properties of multimode squeezed states. Experiment[8] has shown that a squeezed state can be generated in a single transit across a nonlinear medium. The absence of a selective resonator or waveguide is then one of the conditions for multimode squeezing.

The phenomena observed during homodyne detection of multimode squeezed states, which were investigated in this review, are closely related to holographic measurements. Detection with noise below the shot intensity distribution on the surface of detection, as in the case of interference of PS waves with the classical homodyne wave, is nothing but the writing of a hologram of the PS waves, but with a result that is paradoxical from the standpoint of classical electrodynamics. The modulation of "blackening" in space, which is produced by a hologram of this type, is not in general superimposed, as is usual, on the Poisson (shot) photon counting noise, but is subtracted from it, and this may be accompanied by the suppression of noise and the

appearance of uniform illumination as the degree of squeezing increases.

---

[1] We consider a set of PS waves propagating within a small range of directions with the same polarization, and will ignore the crystal anisotropy.

[2] We neglect the change in the field across the boundary between vacuum and the crystal.

[3] In the isotropic case, the spectrum actually depends on the wave number q.

[4] We assume that the spot illuminated by the pump and homodyne waves is large, and that all the results refer to the near zone (in the sense of diffraction) on the area S of the spot.

[5] To be specific, we consider angle and frequency degenerate phase matching $\bar{\theta}(0,0) = \pm \pi/2$.

---

[1] R. E. Slusher, L. W. Holberg et al., Phys. Rev. Lett. 55, 2409 (1985).

[2] Wu Ling-An, J. H. Kimble et al., Phys. Rev. Lett. 57, 2520 (1986).

[3] R. M. Shelby, S. H. Perlmutter et al., Phys. Rev. Lett. 57, 691 (1986).

[4] B. L. Schumaker, R. M. Shelby et al., Phys. Rev. Lett. 58, 357 (1987).

[5] M. G. Raizen, H. J. Kimble, and L. A. Orozco, Phys. Rev. Lett. 59, 198 (1987).

[6] Min Xiao, Wu Ling-An, and H. J. Kimble, Phys. Rev. Lett. 59, 278 (1987).

[7] P. Grangier, R. E. Slusher et al., Phys. Rev. Lett. 59, 2153 (1987).

[8] R. E. Slusher, P. Grangier, A. LaPorta et al., Phys. Rev. Lett. 59, 2566 (1987).

[9] D. F. Walls, Nature 306, 141 (1983).

[10] Y. Yamamoto and H. A. Haus, Rev. Mod. Phys. 58, 1001 (1986).

[11] D. F. Smirnov and A. S. Troshin, Usp. Fiz. Nauk 153, 233 (1987) [Sov. Phys. Usp. 30, 851 (1987)].

[12] J. Opt. Soc. Amer. B 4, 10 (1987).

[13] C. M. Caves, Phys. Rev. D 26, 1817 (1982).

[14] C. M. Caves and B. L. Schumaker, Phys. Rev. A 31, 3068 (1985).

[15] B. Yurke, Phys. Rev. A 32, 300 (1985).

[16] M. D. Levenson, R. M. Shelby, A. Aspect et al., Phys. Rev. A 32, 1550 (1985).

[17] C. M. Caves and D. D. Crough, J. Opt. Soc. Am. B 4, 1535 (1987).

[18] M. I. Kolobov and I. V. Sokolov, Opt. Spektrosk. 66, 753 (1989) [Opt. Spectrosc. (USSR) 66, 440 (1989)].

[19] D. N. Klyshko, Photons and Nonlinear Optics [in Russian], Nauka, Moscow, 1980.

[20] D. N. Klyshko, Zh. Eksp. Teor. Fiz. 94, 88 (1988) [Sov. Phys. JETP 67, 915 (1988)].

[21] A. A. Malygin, A. N. Penin, and A. V. Sergienko, Dokl. Akad. Nauk USSR 281, 308 (1985) [Sov. Phys. Dokl. 30, 229 (1985)].

[22] M. Le Berre-Rousseau, E. Ressayre, and A. Tallet, Phys. Rev. Lett. 43, 1314 (1979).

[23] H. P. Yuen and J. H. Shapiro, IEEE Trans. Inf. Theory 24, 657 (1978).

[24] Z. Bialynicka-Birula and I. Bialynicka-Birula, J. Opt. Soc. Am. B 4, 1621 (1987).

[25] S. A. Akhmanov, A. V. Belinskiĭ, and A. S. Chirkin, Kvant. Elektron. (Moscow) 15, 873 (1988) [Sov. J. Quantum Electron. 15, 560 1988].

[26] S. A. Akhmanov, Y. E. D'yakov, and A. S. Chirkin, Introduction to Statistical Optics and Radiophysics [in Russian], Nauka, Moscow, 1981.

[27] I. V. Sokolov, Zh. Eksp. Teor. Fiz. 72, 1687 (1977) [Sov. Phys. JETP 45, 884 (1977)].

[28] D. N. Klyshko, ibid. 94, 82 (1988) [67, 1131 (1988)].

[29] C. M. Caves, Phys. Rev. D 23, 1693 (1981).

[30] M. I. Kolobov and I. V. Sokolov, Zh. Eksp. Teor. Fiz. 90, 1889 (1986) [Sov. Phys. JETP 63, 1105 (1986)].

Translated by S. Chomet

1104   Sov. Phys. JETP 69 (6), December 1989

M. I. Kolobov and I. V. Sokolov   1104